JACS
JOURNAL OF THE AMERICAN CHEMICAL SOCIETY

COMMUNICATION

pubs.acs.org/JACS

Kinetic Separation of Propene and Propane in Metal−Organic Frameworks: Controlling Diffusion Rates in Plate-Shaped Crystals via Tuning of Pore Apertures and Crystallite Aspect Ratios

Chang Yeon Lee,[†,∥] Youn-Sang Bae,[‡,∥] Nak Cheon Jeong,[†] Omar K. Farha,[†] Amy A. Sarjeant,[†] Charlotte L. Stern,[†] Peter Nickias,[§] Randall Q. Snurr,[*,‡] Joseph T. Hupp,[*,†] and SonBinh T. Nguyen[*,†]

[†]Department of Chemistry and [‡]Department of Chemical and Biological Engineering, Northwestern University, 2145 Sheridan Road, Evanston, Illinois 60208, United States

[§]The Dow Chemical Company, Core R&D, 1776 Building, Midland, Michigan 48674, United States

Supporting Information

ABSTRACT: A series of isostructural, noncatenated, zinc-pillared-paddlewheel metal−organic framework materials has been synthesized from 1,2,4,5-tetrakis(carboxyphenyl)benzene and *trans*-1,2-dipyridylethene struts. Substantial kinetic selectivity in the adsorption of propene over propane can be observed, depending on the pore apertures and the rectangular-plate morphology of the crystals.

Highly porous metal−organic frameworks (MOFs)[1] are receiving increasing attention because of their promise in a wide variety of applications such as gas and chemical storage,[2] chemical separations,[3] sensing,[4] selective catalysis,[5] ion exchange,[6] and drug delivery.[7] Although MOFs have been touted as having great potential in gas separations and the purification of gas mixtures by adsorption, most studies to date have focused on the adsorption behavior of only simple gases such as H_2, CO_2, and CH_4. Selective separation of olefins from paraffins, an important industrial process, has been investigated using MOFs in only a few papers, which have reported either thermodynamic[8] or kinetic selectivity.[9] For example, Li et al.[9] reported highly promising kinetic selectivity in MOFs having small pore apertures that allow the smaller propene molecules to enter the pores faster than the larger propane molecules (selectivity = 125 favoring propene).

The separation of olefins and paraffins having the same number of carbon atoms is an intrinsically difficult problem because of the similar physicochemical properties of these compounds. Successful separation has relied on energy-intensive and costly cryogenic distillation as the mainstay technology in the petrochemical industry for the last 70 years.[10] Because adsorption separations tend to be more energy efficient than distillations, there is tremendous interest in developing adsorbents that could be used to separate olefins and paraffins. In this paper, we report a modularly tunable series of MOFs whose pore opening sizes can be tuned to probe the effect of aperture size on adsorption selectivity. While we uncovered a significant kinetic selectivity for propene over propane in this system as the pore opening decreases, this parameter is not solely responsible for the observed selectivity; the shape of the MOF crystals and the manner in which the internal pore channels are oriented with respect to the crystal faces also contribute significantly.

Previously, our groups have reported the synthesis of **TO** MOF, a noncatenated, pillared, paddlewheel MOF made up of two struts, a *t*rimethylsilane (TMS)-protected, acetylene-containing dipyridyl strut **L4** and an *o*ctaoxygenated strut **L1**, held together with Zn^{2+} nodes.[11] This material can be isolated as thin rectangular plates with high length-to-thickness and width-to-thickness ratios favoring the plane containing the octadentate strut **L1**. From the view normal to this plane (i.e., along the direction of the dipyridyl strut **L4**), it is evident that two types of channels, ***I*** and ***II***, are available in the MOF crystal (see Figure 1). The aperture for channel ***II*** can be readily narrowed via 3,6-functionalization of **L1** (e.g., with bromine atoms to give the octaoxygenated dibrominated strut **L2**).[12] In this manner, the effect of pore aperture size on the kinetic separation of propene and propane can be tested. Incorporation of the easily removed TMS protecting group into the pillared strut **L4** allowed us to probe the effect of pore congestion.

The synthesis of all four MOFs is depicted in Scheme 1. **DTO**, **DBTO**, and **BTO** MOFs (**B** indicates a composition that includes the di*b*rominated strut **L2** and **D** indicates a composition that includes the *d*eprotected acetylene-containing strut **L3**) were successfully synthesized solvothermally using $Zn(NO_3)_2 \cdot 6H_2O$ and the appropriate combinations of struts (**L1** and **L3**, **L2** and **L3**, and **L2** and **L4**, respectively).

Single-crystal X-ray diffraction (XRD) confirmed that **DTO**, **DBTO**, and **BTO** MOFs are noncatenated, pillared-paddlewheel frameworks that are isostructural with **TO** MOF. All three new MOFs were isolated as highly anisotropic plates that are thin along the direction of the dipyridyl ligands (**L3** or **L4**), mirroring the morphology of **TO**. Powder XRD data [Figure S1 in the Supporting Information (SI)] for all four materials revealed strong peaks corresponding to the direction of the dipyridyl pillars, indicating that the majority of the crystals lie flat in the sample holder, with the plane containing the octadentate ligands (**L1** or **L2**) being perpendicular to the incident X-ray beam.

Thermogravimetric analysis data for the as-synthesized samples of **DTO**, **TO**, **DBTO**, and **BTO** MOFs indicated high porosity (40−45%; see Figure S2). CO_2 adsorption−desorption measurements at 273 K for activated (i.e., solvent-evacuated) samples of all four MOFs yielded type-I isotherms (Figure S3),

Received: January 27, 2011
Published: March 18, 2011

dx.doi.org/10.1021/ja200553m | *J. Am. Chem. Soc.* 2011, 133, 5228–5231

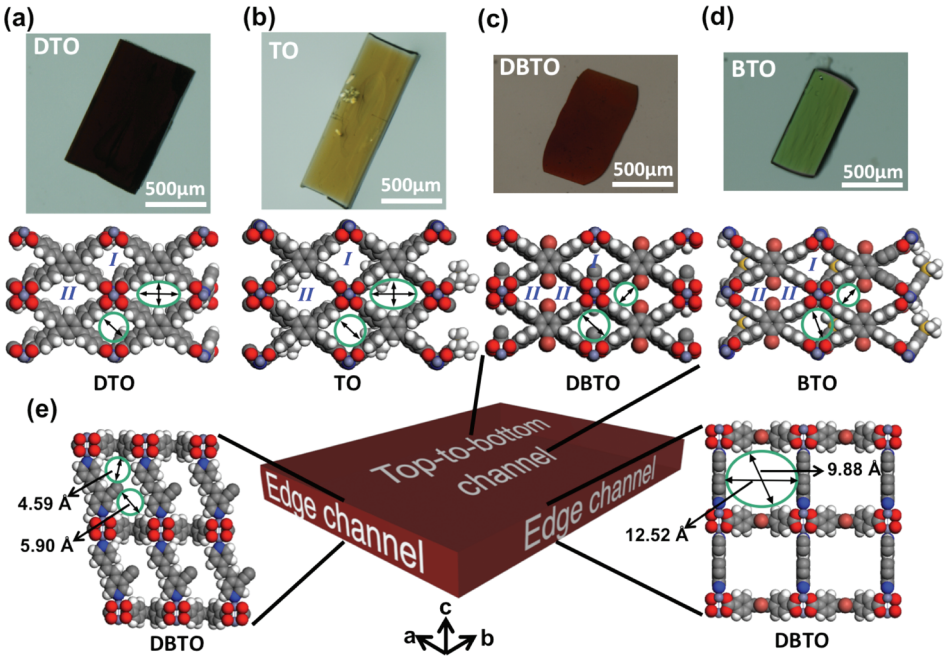

Figure 1. (a–d) Microscope images (top of each panel) and crystal packing diagrams (bottom of each panel) of the four isostructural MOFs, showing the pores running along the dipyridyl struts **L3** and **L4**: (a) **DTO**, (b) **TO**, (c) **DBTO**, (d) **BTO**. We note that the Br atoms in **L2** effectively bisect channel *II* in **DTO** MOF into two smaller channels in **DBTO** MOF. (e) Crystal packing diagrams of **DBTO** MOF showing the framework pores along the (right) *a* and (left) *b* axes.

Scheme 1. Synthesis of the Isostructural MOFs DTO, TO, DBTO, and BTO[a]

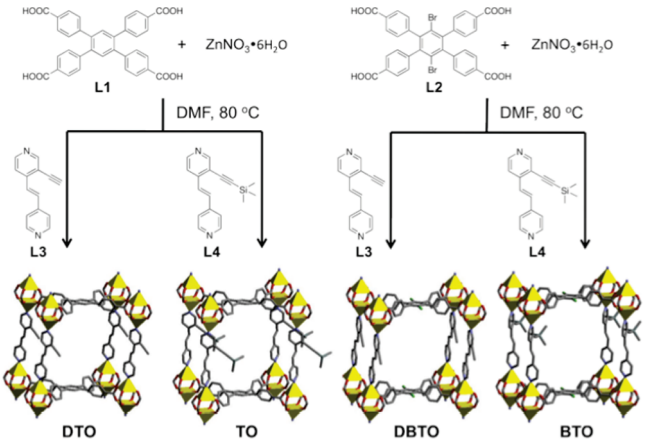

[a] The stick representation of the unit cell for each MOF is shown (yellow polyhedra = Zn, red = O, green = Br, blue = N, gray = C). Solvent molecules, hydrogen atoms, and disordered atoms have been omitted for clarity. For larger illustrations of the structures, please see the SI.

indicating microporosity. Nonlinear density functional theory (NLDFT) surface area data (Table 1) were consistent with a decrease in specific surface area in the order **DTO** > **TO** > **DBTO** > **BTO** due to the presence of TMS and Br groups. The pore volumes and apertures of channels *II* (Table 1 and Figure 1) are ordered in the same manner, with those in **DTO** and **TO** MOFs (4.26–5.70 and 4.88–6.03 Å, respectively) being much larger than those in **DBTO** and **BTO** MOFs (3.34 and 3.05 Å). Additionally, notable decreases in the aperture size of channel *I* were also observed in **DBTO** and **BTO** MOFs as a result of pore shrinkage due to an increasing angle between the two phenyl rings in **L2** to avoid steric hindrance with the large bromine atom. Taken together, these data support our hypothesis that systematic modification of the struts in an isostructural series of frameworks can result in rational tuning of the internal surface area, the micropore volume, and the aperture of a channel/pore.

The ability of **DTO**, **TO**, **DBTO**, and **BTO** MOFs to take up propene and propane was evaluated via single-component isotherms measured volumetrically at 298 K on activated samples of each MOF. For both gases, these isotherms showed saturation at 3–4 bar, and the saturated adsorbed amounts (Figure S5) followed the order of surface areas and micropore volumes (**DTO** > **TO** > **DBTO** > **BTO**). **DTO** MOF with no TMS or Br moieties, has the largest pore volume and can take up ~3 times as much propene and propane as **BTO** MOF, whose micropore volume is ~2.4 times smaller.

Qualitatively, the kinetic selectivity in the adsorption of propene versus propane by **DTO**, **TO**, **DBTO**, and **BTO** MOFs can be deduced from the time-dependent gas uptake profiles (Figure 2). **DBTO** and **BTO** MOFs showed similar kinetic selectivities, with considerably faster uptake of propene than propane. In contrast, **TO** and **DTO** MOFs constructed using the nonbrominated ligand **L1** did not show such large differences in the propene versus propane adsorption kinetics. These observations can be explained qualitatively by the thin-rectangular-plate morphology of the MOF crystals (Figure 1), which naturally favors the flow of gas through the *I* and *II* channels that run parallel to the dipyridyl struts (see discussion above) and terminate on the largest crystal faces (i.e., the top-to-bottom channels). While other kinds of channels terminate on pairs of edge faces, the combined area of the four edge faces is much smaller than that of the top and bottom faces, making the fluxes through the edge channels minor contributors (despite the larger apertures for these channels; see

dx.doi.org/10.1021/ja200553m |*J. Am. Chem. Soc.* 2011, 133, 5228–5231

Table 1. Surface Areas, Micropore Volumes, and Aperture Sizes for DTO, TO, DBTO, and BTO MOFs

			aperture size (Å)[b]	
MOF	CO_2 surface area (m^2/g)[a]	micropore volume (cm^3/g)[a]	channel *I*	channel *II*
DTO	669	0.24	5.27	4.26−5.70
TO	512	0.18	5.39	4.88−6.03
DBTO	457	0.17	5.10	3.34
BTO	283	0.10	4.67	3.05

[a] Calculated using NLDFT. [b] Calculated from the single-crystal X-ray structures of **DTO**, **TO**, **DBTO**, and **BTO** MOFs, taking the van der Waals radii of the MOF atoms into account. See Figure 1a−d for illustrations of the aperture sizes.

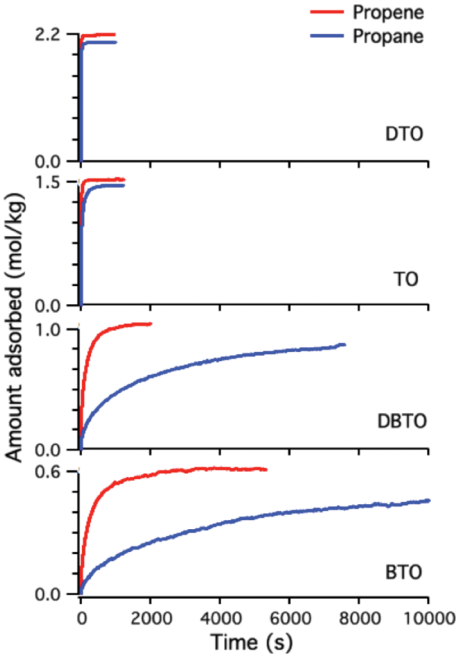

Figure 2. Time-dependent propene and propane uptake profiles for **DTO**, **TO**, **DBTO**, and **BTO** MOFs at 0.3 bar and 298 K.

Figure 1e). In view of this information about the crystal morphology, the large kinetic selectivities for propene over propane by **DBTO** and **BTO** MOFs are best attributed to the reduction in the apertures for channels ***I*** and ***II*** (Table 1), a consequence of the Br atoms of the **L2** ligands. Because C_3H_6 is (slightly) smaller than C_3H_8,[13] this restriction would naturally increase the kinetic selectivity for the olefin.

The kinetic selectivity for the adsorption of propene over propane by a solid can be defined as the ratio of the two gases' diffusional time constants (given by D/r^2, where D is the diffusion coefficient and r is a characteristic length scale as defined in the SI).[14] As shown in Table 2, this ratio increases in the order **DTO** < **TO** ≪ **DBTO** < **BTO**. The much larger kinetic selectivities displayed by the **DBTO** and **BTO** MOFs relative to the **DTO** and **TO** materials are qualitatively consistent with the corresponding differences in aperture size for channels ***I*** and ***II***. That is, as the pore aperture becomes more constricted, the kinetic selectivity for propene over propane greatly increases.

Table 2. Kinetic Selectivities for the Uptake of Propene over Propane in the Activated DTO, TO, DBTO, and BTO MOFs, Expressed as the Ratio of the Two Relevant Diffusion Time Constants (D/r^2); Also Included for Comparison Are the Values for a Sample of Activated DBTO MOF That Had Been Ground into Smaller Crystals

entry	material	gas	D/r^2 (s^{-1})	kinetic selectivity
1	**DTO**	propene	1.1×10^{-2}	1.4
		propane	8.1×10^{-3}	
2	**TO**	propene	4.2×10^{-3}	2.5
		propane	1.7×10^{-3}	
3	**DBTO**	propene	3.3×10^{-4}	11
		propane	2.9×10^{-5}	
4	**BTO**	propene	1.3×10^{-4}	12
		propane	1.1×10^{-5}	
5	ground **DBTO**	propene	4.2×10^{-3}	3.8
		propane	1.1×10^{-3}	

In contrast, the TMS group, which modulates the widths of channels terminating at the low-area crystal faces (i.e., the edge faces; see Figure 1e), plays almost no role in determining the kinetic selectivities of the MOFs constructed from **L2** and only a small role (a factor of ∼1.7) in determining the relative selectivities of those constructed from **L1**. By referencing transport in **DTO** MOF, we find that the TMS group in **TO** MOF attenuates the diffusion time constant of propane by a factor of 4.7 but reduces the time constant for propene by only a factor of 2.7. In **BTO** MOF, the TMS group reduces the relative time constants for transport of propane and propene essentially equally (by factors of 2.7 and 2.5, respectively) and thus contributes almost nothing to the kinetic selectivity. These last observations indicate that the large bromine atoms in **L2** are the main structural contributor to the kinetic selectivities of **BTO** and **DBTO** MOFs. Thus, differing rates for propene versus propane navigation of the narrowed and shrunken top-to-bottom channels of **BTO** and **DBTO** MOFs are what account for the large (∼12-fold) kinetic selectivities of these materials.

Interestingly, when the single-component isotherms for propene and propane for each of the four MOFs were compared against each other over the 0−3.5 bar pressure range (Figure S6), none showed significant *thermodynamic* selectivity. These findings imply that specific chemical interactions between TMS or Br and either of the penetrants are absent. Instead, the interactions are only steric.

Despite the substantially larger apertures for the channels aligned in the *a* and *b* directions (i.e., the edge-terminating channels, with aperture sizes of 4.59−5.90 and 9.88−12.52 Å, respectively; see Figure 1e) than for those in the *c* direction (i.e., the top-and-bottom-terminating channels, with aperture sizes of 5.10 Å for channel ***I*** and 3.34 Å for channel ***II***; Figure 1c), the observed sizable kinetic selectivity for **DBTO** MOF is obtained because the characteristic times for traversing the **DBTO** MOF crystallites in both the *a* and *b* directions are much greater than those in the *c* direction. This apparent inconsistency can be reconciled by recognizing that the crystallite dimensions (proportional to the diffusion distances) are much longer in the *a* and *b* directions than in the *c* direction (for **DBTO** MOF, the ratio of length to thickness ranges from ∼10 to 21, depending on the particular crystallite examined, while the ratio of width to thickness varies from 6 to 15, as calculated from microscopy images). In other words, the crystallite shape matters (recall that the diffusional

dx.doi.org/10.1021/ja200553m |*J. Am. Chem. Soc.* 2011, 133, 5228–5231

transport time increases as the *square* of the diffusion distance). We reasoned that if the forgoing interpretations were correct, reducing the crystallite size in the *a* and *b* directions but not the *c* direction should diminish the kinetic selectivity (since indiscriminate molecular transport through channels aligned in the *a* or *b* direction should become more significant). To test the idea, we mechanically ground a sample of plate-shaped **DBTO** MOF crystallites (see Figure S9) and then evaluated their propane and propene transport. Indeed, grinding decreased the kinetic selectivity from 11 to 3.8 (entries 3 and 5 in Table 2; also see Figure S7).

In conclusion, we have found that systematic structural modification of the organic struts in a series of MOFs can allow for tuning of the pore apertures (via the introduction of Br atoms) and modulation of channel congestion (via the presence of the TMS group). While both kinds of modification influence the rates of molecular transport, for the systems studied here only the former appreciably affects the propene/propane kinetic selectivity. Although we were fortuitously successful in this endeavor by constricting channels ***I*** and ***II*** with the Br atoms of strut **L2**, our accomplishment cannot be attributed solely to the tuning of aperture dimensions. The thin rectangular shape of the MOF crystals and the fortuitous manner in which the modified channel is oriented perpendicular to the largest faces of the crystals are also necessary for achieving high kinetic selectivities for propene versus propane. Thus, while structural modification of the strut is a critical step in crystal engineering, at least in the present case it must be combined with suitable crystallite morphology in order for high kinetic selectivity to be realized experimentally. In contrast, for systems based solely on thermodynamic selectivity, crystallite morphology generally should not be an important consideration.

■ ASSOCIATED CONTENT

Supporting Information. Synthesis and characterization data for all MOFs, including single-crystal XRD data (CIF); detailed descriptions of the conditions and results of the gas separation experiments; a complete tabulation of the experimental kinetic data plotted in Figure 2 and Figure S7 (XLS); and complete refs 7c and 8d. This material is available free of charge via the Internet at http://pubs.acs.org.

■ AUTHOR INFORMATION

Corresponding Author

snurr@northwestern.edu; j-hupp@northwestern.edu; stn@northwestern.edu

Author Contributions

‖These authors contributed equally.

■ ACKNOWLEDGMENT

We acknowledge the Dow Chemical Company for financial support of this work. Additional support was provided by the U.S. Department of Energy (Grant DE-FG02-03ER15457), the National Science Foundation through the Northwestern NSEC, AFOSR, and DTRA/ARO.

■ REFERENCES

(1) (a) Férey, G. *Chem. Soc. Rev.* **2008**, *37*, 191. (b) Tranchemontagne, D. J.; Mendoza-Cortes, J. L.; O'Keeffe, M.; Yaghi, O. M. *Chem. Soc. Rev.* **2009**, *38*, 1257.

(2) (a) Furukawa, H.; Yaghi, O. M. *J. Am. Chem. Soc.* **2009**, *131*, 8875. (b) Murray, L. J.; Dincă, M.; Long, J. R. *Chem. Soc. Rev.* **2009**, *38*, 1294.

(3) (a) Bae, Y.-S.; Mulfort, K. L.; Frost, H.; Ryan, P.; Punnathanam, S.; Broadbelt, L. J.; Hupp, J. T.; Snurr, R. Q. *Langmuir* **2008**, *24*, 8592. (b) Li, J. R.; Kuppler, R. J.; Zhou, H. C. *Chem. Soc. Rev.* **2009**, *38*, 1477. (c) Bae, Y.-S.; Farha, O. K.; Spokoyny, A. M.; Mirkin, C. A.; Hupp, J. T.; Snurr, R. Q. *Chem. Commun.* **2008**, 4135. (d) Banerjee, R.; Furukawa, H.; Britt, D.; Knobler, C.; O'Keeffe, M.; Yaghi, O. M. *J. Am. Chem. Soc.* **2009**, *131*, 3875. (e) Bae, Y.-S.; Farha, O. K.; Hupp, J. T.; Snurr, R. Q. *J. Mater. Chem.* **2009**, *19*, 2131. (f) Chen, B. L.; Xiang, S. C.; Qian, G. D. *Acc. Chem. Res.* **2010**, *43*, 1115. (g) Chen, B. L.; Ma, S. Q.; Zapata, F.; Fronczek, F. R.; Lobkovsky, E. B.; Zhou, H. C. *Inorg. Chem.* **2007**, *46*, 1233.

(4) (a) Allendorf, M. D.; Bauer, C. A.; Bhakta, R. K.; Houk, R. J. T. *Chem. Soc. Rev.* **2009**, *38*, 1330. (b) Lu, G.; Hupp, J. T. *J. Am. Chem. Soc.* **2010**, *132*, 7832. (c) Kreno, L. E.; Hupp, J. T.; Van Duyne, R. P. *Anal. Chem.* **2010**, *82*, 8042.

(5) (a) Shultz, A. M.; Farha, O. K.; Hupp, J. T.; Nguyen, S. T. *J. Am. Chem. Soc.* **2009**, *131*, 4204. (b) Ma, L. Q.; Abney, C.; Lin, W. B. *Chem. Soc. Rev.* **2009**, *38*, 1248. (c) Lee, J.; Farha, O. K.; Roberts, J.; Scheidt, K. A.; Nguyen, S. T.; Hupp, J. T. *Chem. Soc. Rev.* **2009**, *38*, 1450.

(6) Min, K. S.; Suh, M. P. *J. Am. Chem. Soc.* **2000**, *122*, 6834.

(7) (a) Horcajada, P.; Serre, C.; Vallet-Regi, M.; Sebban, M.; Taulelle, F.; Férey, G. *Angew. Chem., Int. Ed.* **2006**, *45*, 5974. (b) An, J. Y.; Geib, S. J.; Rosi, N. L. *J. Am. Chem. Soc.* **2009**, *131*, 8376. (c) Horcajada, P.; et al. *Nat. Mater.* **2010**, *9*, 172.

(8) (a) Hartmann, M.; Kunz, S.; Himsl, D.; Tangermann, O.; Ernst, S.; Wagener, A. *Langmuir* **2008**, *24*, 8634. (b) Lamia, N.; Jorge, M.; Granato, M. A.; Paz, F. A. A.; Chevreau, H.; Rodrigues, A. E. *Chem. Eng. Sci.* **2009**, *64*, 3246. (c) Maes, M.; Alaerts, L.; Vermoortele, F.; Ameloot, R.; Couck, S.; Finsy, V.; Denayer, J. F. M.; De Vos, D. E. *J. Am. Chem. Soc.* **2010**, *132*, 2284. (d) Yoon, J. W.; et al. *Angew. Chem., Int. Ed.* **2010**, *49*, 5949. (e) Gücüyener, C.; van den Bergh, J.; Gascon, J.; Kapteijn, F. *J. Am. Chem. Soc.* **2010**, *132*, 17704.

(9) Li, K. H.; Olson, D. H.; Seidel, J.; Emge, T. J.; Gong, H. W.; Zeng, H. P.; Li, J. *J. Am. Chem. Soc.* **2009**, *131*, 10368.

(10) Eldridge, R. B. *Ind. Eng. Chem. Res.* **1993**, *32*, 2208.

(11) Gadzikwa, T.; Farha, O. K.; Malliakas, C. D.; Kanatzidis, M. G.; Hupp, J. T.; Nguyen, S. T. *J. Am. Chem. Soc.* **2009**, *131*, 13613.

(12) Farha, O. K.; Malliakas, C. D.; Kanatzidis, M. G.; Hupp, J. T. *J. Am. Chem. Soc.* **2010**, *132*, 950.

(13) Zhu, W.; Kapteijn, F.; Moulijn, J. A. *Chem. Commun.* **1999**, 2453.

(14) Kärger, J.; Ruthven, D. M. *Diffusion in Zeolites and Other Microporous Solids*; Wiley: New York, 1992.